Journal of Power Sources 195 (2010) 4266–4271

Contents lists available at ScienceDirect

Journal of Power Sources

journal homepage: www.elsevier.com/locate/jpowsour

Electrochemical and impedance investigation of the effect of lithium malonate on the performance of natural graphite electrodes in lithium-ion batteries

Xiao-Guang Sun*, Sheng Dai

Chemical Sciences Division, Oak Ridge National Laboratory, One Bethel Valley Road, Oak Ridge, TN 37831, United States

ARTICLE INFO

Article history:
Received 7 January 2010
Accepted 8 January 2010
Available online 18 January 2010

Keywords:
Lithium malonate
Additive
Surface coating
Lithium-ion battery
Coulomb efficiency

ABSTRACT

Lithium malonate (LM) was coated on the surface of a natural graphite (NG) electrode, which was then tested as the negative electrode in the electrolytes of 0.9 M $LiPF_6$/EC–PC–DMC (1/1/3, w/w/w) and 1.0 M $LiBF_4$/EC–PC–DMC (1/1/3, w/w/w) under a current density of 0.075 mA cm^{-2}. LM was also used as an additive to the electrolyte of 1.0 M $LiPF_6$/EC–DMC–DEC (1/1/1, v/v/v) and tested on a bare graphite electrode. It was found that both the surface coating and the additive approach were effective in improving first charge–discharge capacity and coulomb efficiency. Electrochemical impedance spectra showed that the decreased interfacial impedance was coupled with improved coulomb efficiency of the cells using coated graphite electrodes. Cyclic voltammograms (CVs) on fresh bare and coated natural graphite electrodes confirmed that all the improvement in the half-cell performance was due to the suppression of the solvent decomposition through the surface modification with LM. The CV data also showed that the carbonate electrolyte with LM as the additive was not stable against oxidation, which resulted in lower capacity of the full cell with commercial graphite and $LiCoO_2$ electrodes.

1. Introduction

Worldwide environmental concerns have initiated the shift from conventional combustion engine-powered vehicles to electric vehicles (EVs), hybrid-electric vehicles (HEVs), and plug-in hybrid-electric vehicles (PHEVs). As a result, rechargeable lithium-ion batteries have been actively sought for these applications because of their high voltage and high energy density as compared with other rechargeable battery systems such as lead acid, nickel–cadmium, nickel–metal hydride, etc. From the practical point of view, these batteries must meet safety requirements and have long lives (>10 years). To a larger extent, these factors are determined by the quality of the solid electrolyte interface (SEI) formed on the surface of graphite electrodes, since graphite has been used as the standard anode electrode in commercial lithium-ion batteries. It is generally recognized that the SEI forms during the initial several cycles as a result of the decomposition of the electrolytes and that its formation is affected by the electrolyte composition, surface morphology of the graphite, etc. [1,2]. The perfect SEI should be thin and stable enough to prevent electron tunneling while allowing lithium transport and preventing further electrolyte decomposition. However, it has been reported that the SEI layer on graphite/carbon electrodes grows with cycling and storage, which deteriorates the battery performance and shortens its life [3–6]. The SEI formation process causes initial irreversible capacity loss, and the constant crack/repair mechanism of the SEI then leads to continued capacity loss, both of which result in decreased energy density of the batteries. Therefore, designing desirable interfaces/interphases (SEI) that will cause minimal initial irreversible capacity loss and prevent gradual capacity loss over time is a major scientific challenge that must be met to achieve truly innovative breakthroughs in future chemical energy storage devices.

Different approaches have been used to limit the initial irreversible capacity as low as possible [7–23]. Since the initial irreversible capacity loss is closely related to the surface area of the graphite [2], much effort has been expended in attempts to modify the surface of graphite, such as coating with ionic conducting polymers [8,14], zirconia [9,12], carbon [10,16,19], Li_2CO_3 [11], oxalatoborate [17], alkali [18], and mild oxidation [13]. Sacrificial additives such as CO_2 [20], SO_2 [21], and vinylene carbonate [22,23] have also been used to improve the surface properties. In this study we investigated the effect of simple organic lithium salt, lithium malonate (LM), on the performance of the graphite electrode, especially the initial irreversible capacity and coulomb efficiency. Different techniques such as cyclic voltammetry, charge and discharge, and electrochemical impedance spectroscopy were used for this study.

* Corresponding author. Tel.: +1 865 241 8822; fax: +1 865 576 5235.
E-mail address: sunx@ornl.gov (X.-G. Sun).

0378-7753/$ – see front matter © 2010 Elsevier B.V. All rights reserved.
doi:10.1016/j.jpowsour.2010.01.024

2. Experimental

Lithium foil, lithium hydroxide, malonic acid, 1-methyl-2-pyrolidinone, methanol, carbon black, and polyvinylidene fluoride were all obtained from Aldrich and were used as supplied. Natural graphite from Pred Materials and copper foil from Storm copper component Co. were used as obtained. Deionized H_2O was obtained via the use of a Millipore ion-exchange resin deionizer. Lithium hexafluorophosphate ($LiPF_6$) and lithium tetrafluoroborate ($LiBF_4$) from Aldrich were dried under vacuum at 80 °C for 12 h. Ethylene carbonate (EC), propylene carbonate (PC, anhydrous), dimethyl carbonate (DMC, anhydrous), and diethyl carbonate (DEC, anhydrous) were obtained from Aldrich and were stored over 4 A molecular sieves before use. The water content in the carbonate mixture was below 10 ppm as determined by Karl Fisher's titration. The electrolytes selected for study were 1.0 M $LiBF_4$/EC–PC–DMC (1/1/3, w/w/w), 0.9 M $LiPF_6$/EC–PC–DMC (1/1/3, w/w/w), and 1.0 M $LiPF_6$/EC–DMC–DEC (1/1/1, v/v/v).

Lithium malonate (LM) was synthesized by neutralizing malonic acid with lithium hydroxide. The graphite (95 wt%) was coated onto copper foil by using polyvinylidene fluoride (PVdF) as binder and 1-methyl-2-pyrolidinone (NMP) as solvent. The casted graphite electrode was treated with a dilute solution of 0.02 M LM in methanol/H_2O. The graphite electrode was dipped into the solution and immediately removed. After drying in the oven at 100 °C, the electrode was treated again and finally dried and pressed under a hydrolytic pressure of 1 t for 1 min. The graphite electrodes were all cut into discs with areas of 2.27 cm^2 and further dried under vacuum at 110 °C for 20 h.

Lithium/graphite coin cells were assembled inside an argon-filled glove box with Celgard 2320 as separator. A Maccor Series 4000 tester was used for cell cycling. The cells were cycled between 2.0 and 0.01 V under a current density of 0.15 or 0.075 mA cm^{-2}. Full cells using a commercial graphite electrode with a rated capacity of 1.6 mAh cm^{-2} and a $LiCoO_2$ electrode with a rated capacity of 1.5 mAh cm^{-2} from Pred Materials were assembled and tested between 3.0 and 4.2 V under different current densities. Cyclic voltammetry (CV) was performed by using either platinum or graphite as the working electrode and lithium metal as both the counter and the reference electrodes. The scan rate was set at 1 mV s^{-1}. The cell impedance spectra were measured via a Gamry instrument in the frequency range of 3×10^5 to 1×10^{-3} Hz with perturbation amplitude of 5 mV. The morphological features of the graphite electrode before and after surface coating were observed using scanning electron microscopy (SEM) (JOEL JSM 6060).

3. Results and discussion

3.1. Surface coating of graphite electrodes

The electrode was coated by the dipping method, that is, merging the graphite electrode into the dilute solution of 0.02 M LM in the mixture of methanol/H_2O (3/7, v/v), removing it, and then drying it in an oven at 100 °C. The process was repeated twice, and finally the electrode was pressed under a load of 1 t for 1 min and dried under vacuum at 110 °C for 24 h.

To check the effectiveness of the above-described coating process, one graphite electrode was loaded onto the surface of the SEM holder by copper tape. An SEM image of the electrode was taken, after which LM was coated on its surface via the above coating protocol. After the electrode was dried at 110 °C under vacuum, a second image was taken. Fig. 1a and b shows the SEM images of the graphite electrodes before and after coating, respectively. Before the coating, the sporadic spots on the surface of the graphite electrode can be observed clearly (Fig. 1a). However, after coating

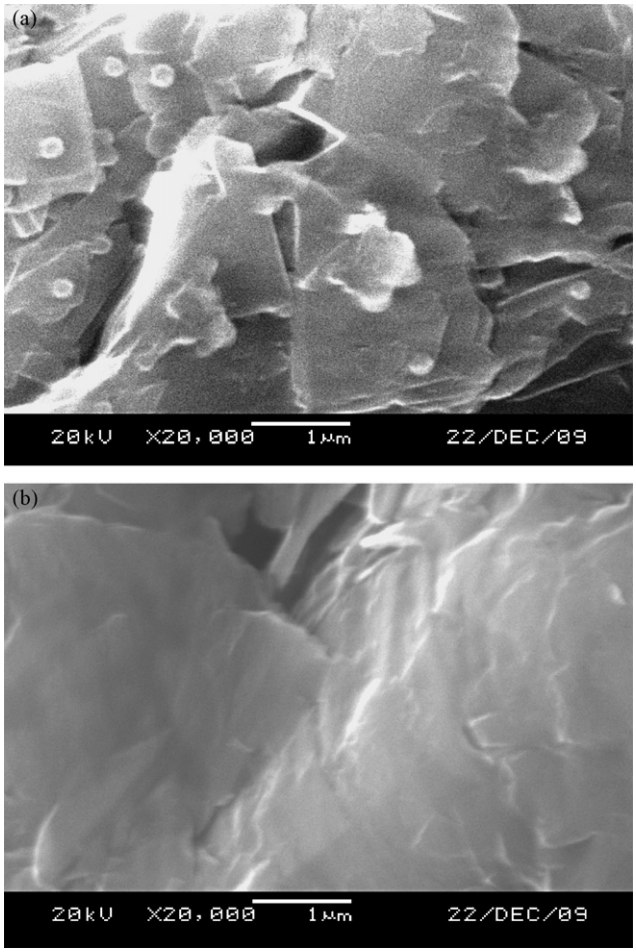

Fig. 1. SEM images of the natural graphite electrodes: (a) before and (b) after surface coating with LM.

such features cannot be observed under the same magnification (Fig. 1b). Instead, the surface appears very smooth. This finding indicates that the surface is indeed modified by the coating process, which is also evidenced by the following half-cell tests and CV measurements.

3.2. Initial charge–discharge behavior of modified natural graphite

The galvanostatic first discharge–charge cycles for the bare and LM-modified natural graphite electrodes were carried out under the current density of 0.075 mA cm^{-2} in the potential range of 0.01 and 2 V vs. Li/Li^+. Fig. 2a shows the first discharge–charge cycles for bare and surface-treated natural graphite electrodes under the current density of 0.075 mA cm^{-2} in 0.9 M $LiPF_6$/EC–PC–DMC (1/1/3 wt%) electrolyte. The initial discharge capacity of the bare NG is 383 mAh g^{-1} and the charge capacity is 320 mAh g^{-1}, which results in a coulomb efficiency of 83.6% for the first cycle. The LM-coated NG delivers 376 mAh g^{-1} of discharge capacity and 321 mAh g^{-1} of charge capacity with a coulomb efficiency of 85.4%. Fig. 2b shows the first discharge–charge cycles for bare and surface-treated natural graphite electrodes under the current density of 0.075 mA cm^{-2} in 1.0 M $LiBF_4$/EC–PC–DMC (1/1/3 wt%) electrolyte. The initial discharge capacity of the bare NG is 369 mAh g^{-1} and the charge capacity is 272 mAh g^{-1}, which results in a coulomb efficiency of 73.7% for the first cycle. The LM-coated NG delivers 359 mAh g^{-1} of discharge capacity and 291 mAh g^{-1} of charge capacity with a coulomb efficiency of 81.1%. Even though there is

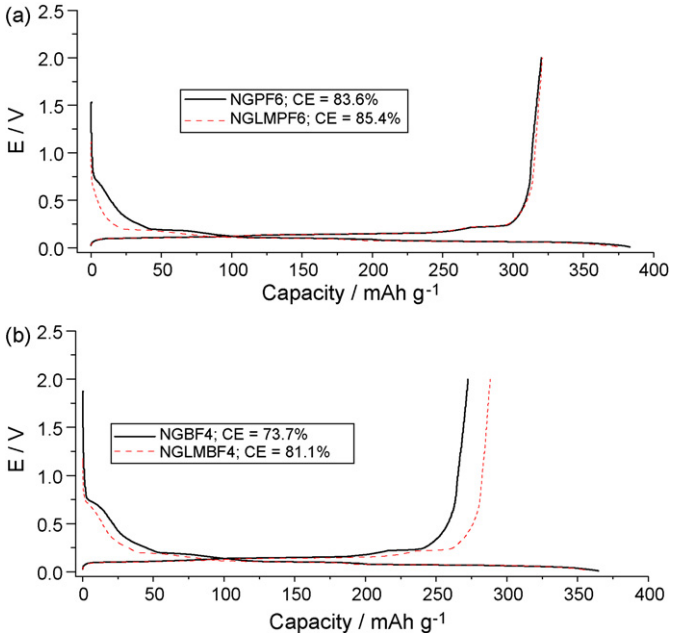

Fig. 2. Initial charge–discharge curves for bare natural graphite and LM-coated graphite electrodes in electrolytes of (a) 0.9 M $LiPF_6$/EC–PC–DMC (1/1/3, w/w/w) and (b) 1.0 M $LiBF_4$/EC–PC–DMC (1/1/3, w/w/w), both tested under a current density of 0.075 mA cm^{-2}.

a difference in the capacity and coulomb efficiency of $LiPF_6$ and $LiBF_4$ solutions, one common feature is noted in the intercalation curve for the LM-modified NG electrode: that is, the shorter plateau around 0.75 V, which is related to the solvent decomposition. These results clearly indicate that the surfaces coated with LM indeed block some reaction sites, which results in reduced irreversible capacity and improved coulomb efficiency.

To better evaluate the salt effect on the initial irreversible capacity and coulomb efficiency, LM was also added to the standard electrolyte of 1.0 M $LiPF_6$/EC–DMC–DEC (1/1/1, v/v/v) with different concentrations such as 0.1, 0.2, and 0.3 wt%, which is relative to the total weight of the electrolyte. However, after more than 1 week, only the electrolyte with 0.1 wt% LM was dissolved completely. For simplicity this electrolyte was used for the cell test. As shown in Fig. 3, the initial discharge capacity of the bare NG is 337 mAh g^{-1} and the charge capacity is 307 mAh g^{-1}, which results in a coulomb efficiency of 91.1% for the first cycle. On the other hand, the cell with 0.1 wt% LM as an additive delivers 353 mAh g^{-1} of discharge capacity and 331 mAh g^{-1} of charge capacity with a coulomb efficiency of 93.8%. This improvement in both the first charge–discharge capacities and the coulomb efficiency is due to the suppressive effect of the salts on solvent decomposition [15], which is evidenced by the initial lower voltage profile during the first lithium intercalation [18] and also supported by the cyclic voltammetry data shown later.

All the tests done in this study using a bare NG electrode yielded plateaus around 0.75 V that are much shorter than those reported in the literature [11,14,17,24]. This finding might be attributable to the difference in graphite sources and its surface properties.

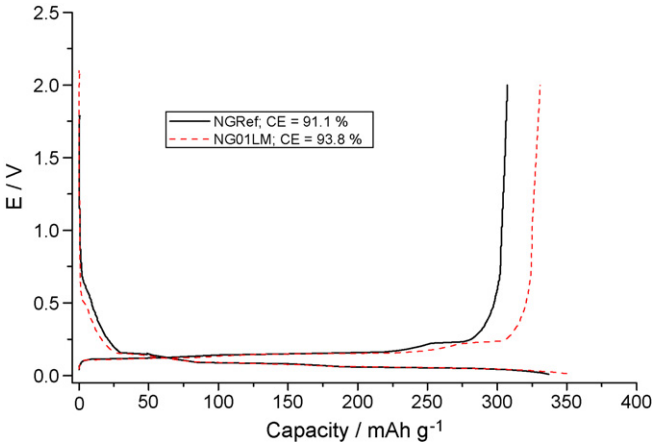

Fig. 3. Initial charge–discharge curves for bare natural graphite electrodes in 1.0 M $LiPF_6$/EC–DMC–DEC (1/1/1, v/v/v) electrolyte, with and without LM as additive, tested under a current density of 0.15 mA cm^{-2}.

3.3. Cyclic voltammograms

To illustrate how the modification of the NG electrode surfaces with LM affects their performance, cyclic voltammetry was performed on fresh bare and LM-modified NGs. Fig. 4a and b shows the CV comparisons of NGs using 0.9 M $LiPF_6$/EC–PC–DMC (1/1/3, w/w/w) and 1.0 M $LiBF_4$/EC–PC–DMC (1/1/3, w/w/w) as electrolytes, respectively. As shown in the figures, there is a reduction peak in the voltage range of 0.2–0.8 V during the cathodic scan in all the CVs of the bare NG. The peak does not appear in the anodic scan, indicating that irreversible reactions are taking place in this potential range. This peak is in the same potential range as the plateau in Fig. 2, confirming that irreversible reactions have occurred during the initial intercalation process. SEI formation and cointercalation of solvated lithium cation [14,24] are likely causes for this phenomenon. The reduction peak in the $LiBF_4$-based solution is more pronounced than that in $LiPF_6$-based solution, indicating that lithium salt has influenced the interfacial reactions [5]. After surface coating with LM, the peaks related to the irreversible reaction are reduced (Fig. 4a and b), indicating that the solvated lithium intercalation reaction is depressed [24], which results in

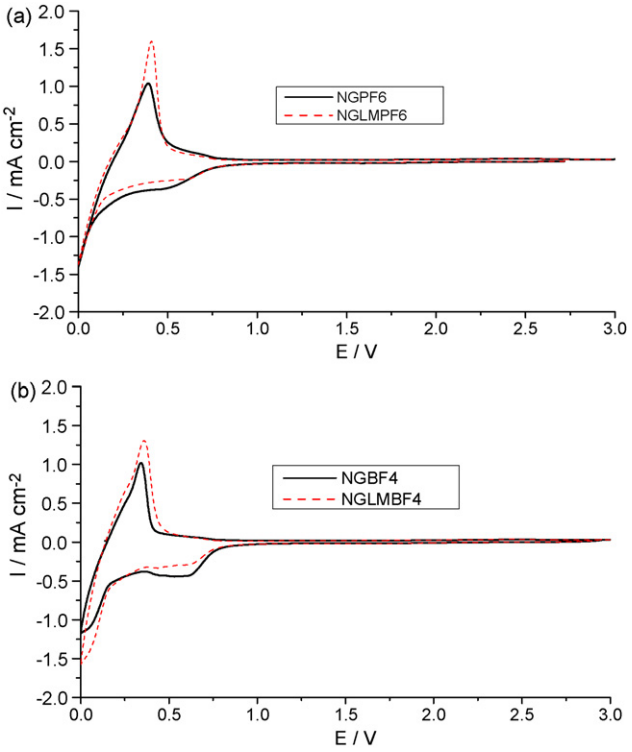

Fig. 4. Cyclic voltammograms for bare natural graphite and LM-coated graphite electrodes in different electrolytes (scan rate of 1 mV s^{-1}): (a) 0.9 M $LiPF_6$/EC–PC–DMC (1/1/3, w/w/w) and (b) 1.0 M $LiBF_4$/EC–PC–DMC (1/1/3, w/w/w).

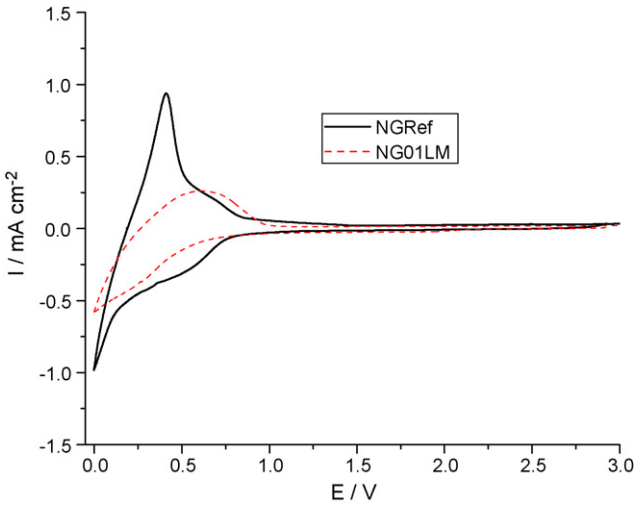

Fig. 5. Cyclic voltammograms for bare natural graphites in 1.0 M $LiPF_6$/EC–DMC–DEC (1/1/1, v/v/v) electrolyte, with and without LM as additive (scan rate of 1 mV s^{-1}).

increased deintercalation capacity and coulomb efficiency (as discussed in the previous section).

Fig. 5 shows the CV comparison of NGs in 1.0 M $LiPF_6$/EC–DMC–DEC (1/1/1, v/v/v) electrolyte, with and without additive LM. Remarkably different from the results of electrode surface coating, the additive in the electrolyte almost totally eliminates the irreversible reduction peak. This result is same as that reported by Choi et al. [15], who used Li_2CO_3 as additive to the electrolyte of 1.0 M $LiPF_6$/EC–DEC (1/1, v/v), which resulted in almost no solvent decomposition on graphite electrode. It is believed that the additive salt [15] is deposited on the surface of the electrode surface before reaching the voltage for solvent decomposition, which results in reduced irreversible capacity and improved coulomb efficiency. Based on the same bulk impedances, as shown in the following section, and the CV differences between using LM as an additive and direct LM coating, it can be concluded that the surface concentration of LM achieved via the additive approach is much higher than that of LM from the direct coating approach.

To check whether the presence of LM in the carbonate has altered the electrochemical window, CVs of the solutions of 1.0 M $LiPF_6$/EC–DEC (1/1, v/v) with and without 0.1 wt% LM have been carried out on platinum electrodes in the voltage range of −0.5 to 5.5 V with lithium as both counter and reference electrodes. As shown in Fig. 6a, the behaviors of lithium deposition/stripping on the Pt electrode are almost the same as those of lithium intercalation/deintercalation on the graphite electrode: that is, the current density of the additive-containing solution is much lower than that of the standard solution. However, on the oxidation side, as shown in Fig. 6b, the opposite trend is observed: that is, the current density of the additive solution is much higher than that of the standard solution, indicating that the additive in the carbonate solution has been oxidized during the anodic scan.

3.4. Impedance spectroscopy

Impedance spectroscopy has been used by various authors [25–31] to analyze cell performance. In order to further understand the cell performance shown in Figs. 2 and 3, their impedance spectra are recorded after two full cycles, which are shown in Figs. 7 and 8, respectively. Generally the impedance spectra of these cells are composed of two merged semicircles and a straight sloping line. The intersection of the impedance spectra with the *x*-axis at the high-frequency end is the bulk resistance (Rb) of the cell, which reflects electrical conductivity of the electrolyte, separator, and electrodes. The semicircle at high frequency is the resistance of the surface layer i.e., the SEI film formed on the surface of the electrodes (R_{SEI}). The semicircle at medium frequencies is the Faradic charge-transfer resistance (R_{ct}). The slope is the Warburg impedance, which is related to the semi-infinite diffusion of lithium ion in the solid electrodes.

The parameters of R_b, R_{SEI}, and R_{ct} from the impedance spectra of Figs. 7 and 8 are obtained via fitting. To facilitate the comparison of each pair, only R_{SEI} and R_{ct} are considered here. For the surface-coating approach, when 0.9 M $LiPF_6$/EC–PC–DMC (1/1/3, w/w/w) is used as electrolyte, the interfacial resistance is increased from 3.0 to 6.0 Ω while the charge-transfer resistance remains 9 Ω (Fig. 7a). When 1.0 M $LiBF_4$/EC–PC–DMC (1/1/3, w/w/w) is used as electrolyte, the interfacial resistance is decreased from 7.5 to 5.5 Ω while the charge-transfer resistance is also decreased from 12.0 to 10.0 Ω (Fig. 7b). For the test using LM as additive, the interfacial resistance remains 1.0 Ω while the charge-transfer resistance is decreased from 12.5 to 5.5 Ω (Fig. 8). It is noted that the decreased interfacial resistance after treatment is always coupled with a large improvement in coulomb efficiency. The exact

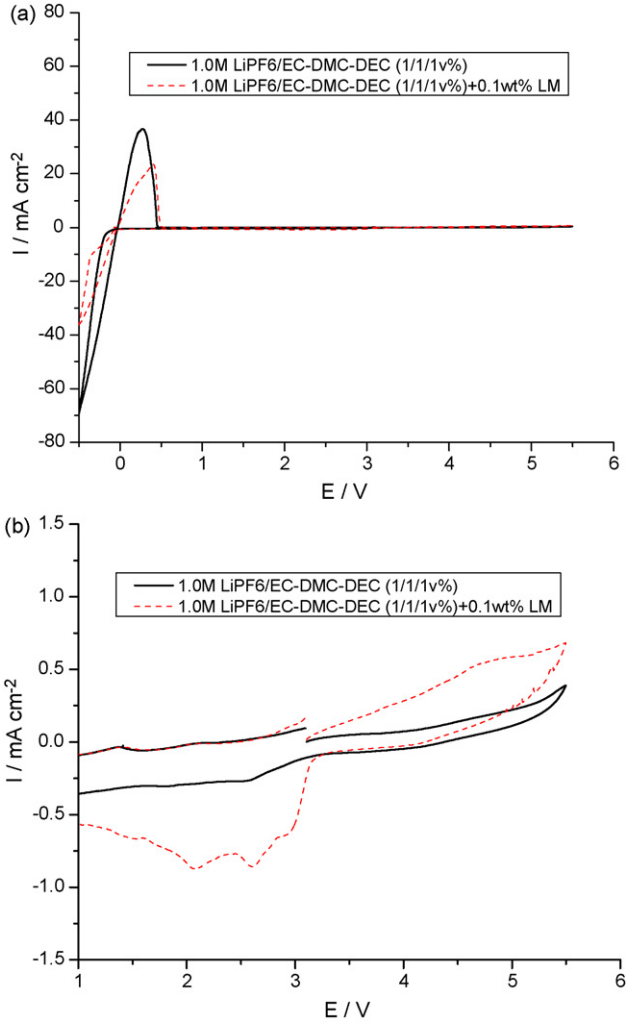

Fig. 6. (a) Electrochemical window of the solution 1.0 M $LiPF_6$/EC–DMC–DEC with and without 0.1 wt% LM (working electrode is Pt; counter and reference electrodes are lithium foil; scan rate is 1 mV s^{-1}). (b) CV segment in the voltage range of 1.0–5.5 V.

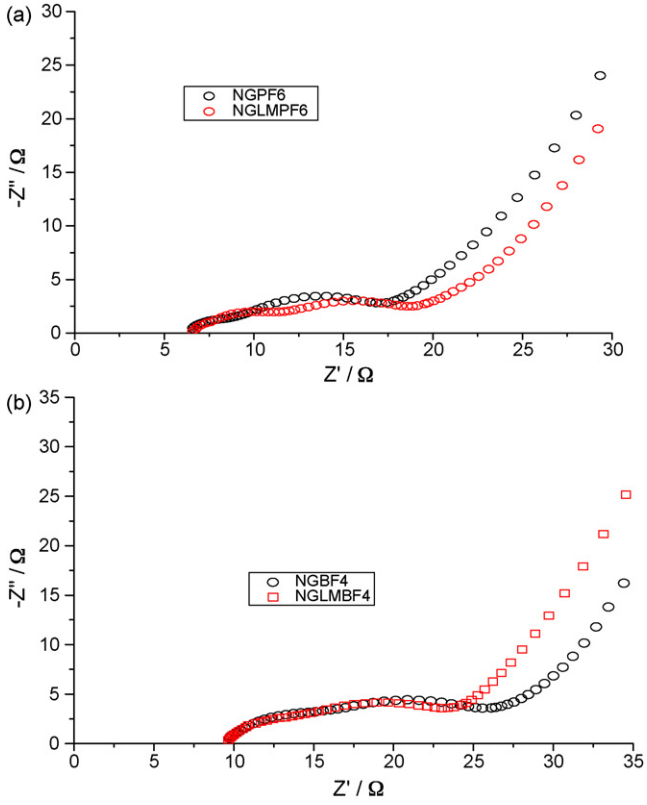

Fig. 7. Impedance spectra of the half-cells in Fig. 1 recorded after two cycles.

reason for this correlation is not clear; however, it is consistent with the published data on using Li_2CO_3 as a suppressant in the carbonate electrolyte [15]. Further experiments are needed to clarify these correlations, and the results will be published in the future.

3.5. Cycling tests

Fig. 9 shows the half-cell cycling data (after the first two formation cycles) of the bare NG and LM-coated NG in the electrolyte of 1.0 M $LiBF_4$/EC–PC–DMC (1/1/3, w/w/w), which have been tested under the current density of 0.075 mA cm^{-2}. With continual cycling, the capacities of both cells decrease and the cell with the surface-coating electrode appears to decrease at a slower pace. It is clear from this cycling test and previous initial-cycle data that the surface LM coating can decrease the initial solvent decompo-

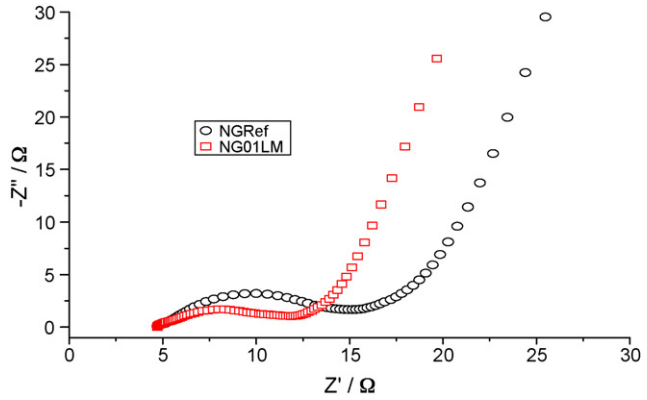

Fig. 8. Impedance spectra of the half-cell in Fig. 2 recorded after two cycles.

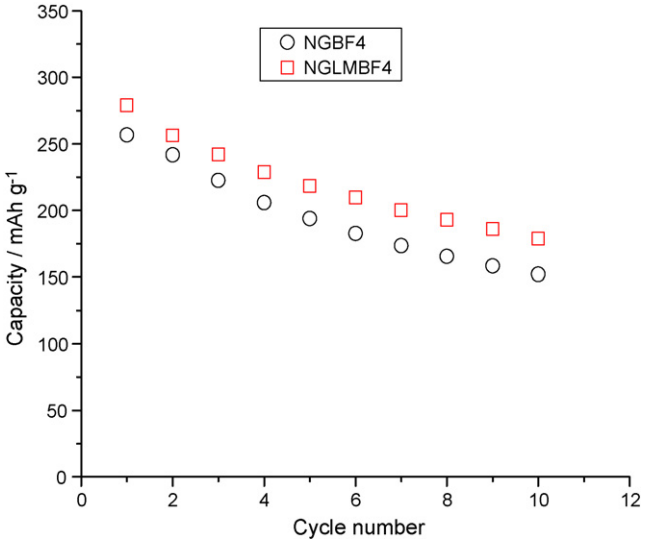

Fig. 9. Cycle performance of the bare natural graphite and LM-coated graphite electrodes in 1.0 M $LiBF_4$/EC–PC–DMC (1/1/3, w/w/w) tested under a current density of 0.075 mA cm^{-2}.

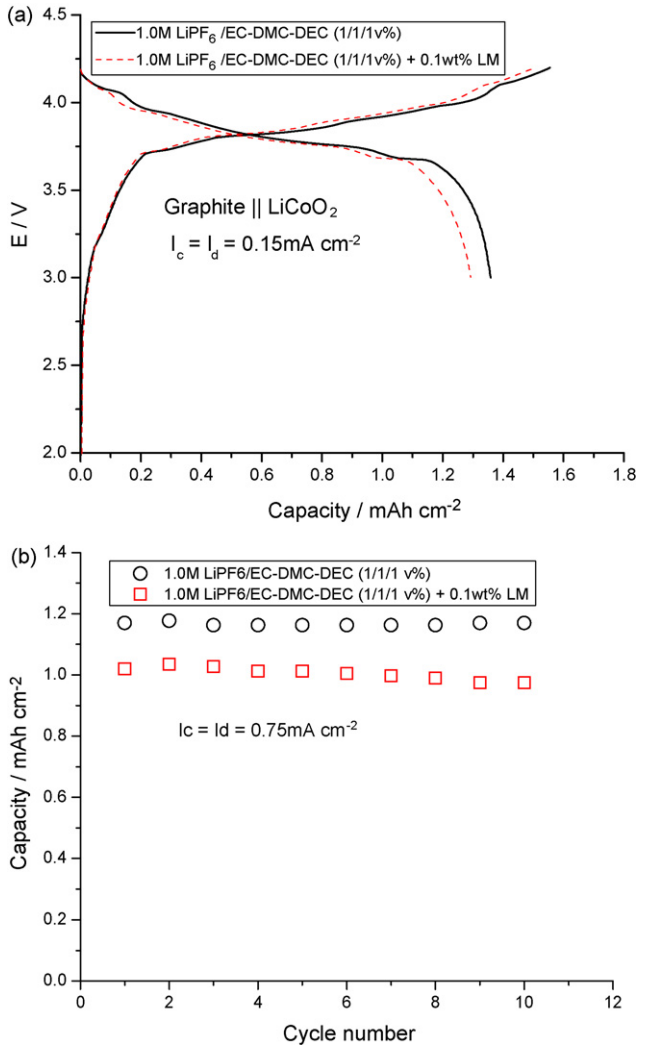

Fig. 10. (a) Initial charge–discharge curves and (b) the cycle performance of the full cell, with graphite and $LiCoO_2$ electrodes, and using 1.0 M $LiPF_6$/EC–DMC–DEC (1/1/1, v/v/v) electrolyte, with and without LM as additive, tested under different current densities.

sition, which results in reduced initial irreversible capacity and improved coulomb efficiency. However, this coating cannot prevent the decrease in capacity with repeated cycling. This implies that the simple LM salt coating might be inadequate to completely prevent solvent decomposition with cycling and that additive components such as elastic polymers might be needed to improve strength and function. Further investigation in this area is under way.

Considering the unstable feature of the LM-containing solution on oxidation (Fig. 6), full cells using a commercial graphite electrode with a rated capacity of 1.6 mAh cm^{-2} and a $LiCoO_2$ electrode with a rated capacity of 1.5 mAh cm^{-2} (both from Pred Materials) were assembled. Fig. 10a shows the initial charge–discharge curves of the full cell using 1.0 M $LiPF_6$/EC–DMC–DEC (1/1/1, v/v/v) electrolyte, without and with LM as additive. These cells were tested under the current density of 0.15 mA cm^{-2}, which is equivalent to the C/10 rate. The initial charge–discharge capacities of the reference cell are 1.56 and 1.36 mAh cm^{-2}, while the initial charge–discharge capacities of the cell using the additive are 1.51 and 1.29 mAh cm^{-2}, respectively. The lower capacity of the cell using LM as an additive is clearly related to its oxidation stability at the cathode, and it is also reflected in the cycle performance in Fig. 10b, which was tested under higher current density of 0.75 mA cm^{-2} (C/2).

4. Conclusion

In summary, these preliminary results have demonstrated that the initial irreversible capacity of the graphite electrode can be decreased by coating the electrode surface with lithium malonate (LM). The decrease in irreversible capacity and improvement in coulomb efficiency are caused by suppression of solvent decomposition, which is confirmed by cyclic voltammetry and ac impedance spectroscopy. The improvement in capacity and coulomb efficiency is coupled with the low interfacial resistance of the cell using the modified graphite electrode. However, the simple electrode surface coating with LM could not prevent the decrease in half-cell capacity with continual cycling, even though it showed a slower rate of decrease than that of the cell without surface coating. This finding suggests that other components such as elastic conductive polymers might be required to improve the strength and function when the surface-coating approach is used. The CV of the carbonate solution containing LM as an additive showed that it was not stable against oxidation, which resulted in lower capacity in full-cell testing with commercial graphite and $LiCoO_2$ electrodes. Thus, LM is not suitable for use as an additive to the electrolyte but rather as a coating agent on the surface of the graphite electrode.

Acknowledgements

This work was conducted at the Oak Ridge National Laboratory and supported by the ORNL laboratory-directed research and development (LDRD) grants of D10-036. This work was also partly supported by the ORNL LDRD program under contract No. DE-AC05-00OR22725 with UT-Battelle, LLC. X.G.S thanks Dr. Chao Hui for taking the SEM images.

References

[1] E. Peled, J. Electrochem. Soc. 126 (1979) 2047.
[2] D. Aurbach, A. Zaban, Y. Ein-Eli, Weissman, O. Chusid, B. Markovsky, J. Power Sources 68 (1997) 91.
[3] E.V. Thomas, H.L. Case, D.H. Doughty, R.G. Jungst, G. Nagasubramanian, E.P. Roth, J. Power Sources 124 (2003) 254.
[4] J. Yamaki, H. Takatsuji, T. Kawamura, M. Egashira, Solid State Ionics 148 (2002) 241.
[5] A.M. Anderson, M. Herstedt, A.G. Bishop, K. Edstrom, Electrochim. Acta 47 (2002) 1885.
[6] R. Yazami, Y.F. Reynier, Electrochim. Acta 47 (2002) 1217.
[7] J.S. Shin, C.H. Han, U.H. Jung, S.I. Lee, H.J. Kim, K. Kim, J. Power Sources 109 (2002) 47.
[8] Q.M. Pan, K.K. Guo, L.Z. Wang, S.B. Fang, Electrochem. Solid State Lett. 6 (2003) A265.
[9] I.R.M. Kottegoda, Y. Kadoma, H. Ikuta, Y. Uchimoto, M. Wakihara, J. Electrochem. Soc. 152 (2005) A1595.
[10] H.Y. Lee, J.K. Baek, S.W. Jang, S.M. Lee, S.T. Hong, K.Y. Lee, M.H. Kim, J. Power Sources 101 (2001) 206.
[11] S.S. Zhang, K. Xu, T.R. Jow, Electrochem. Commun. 5 (2003) 979.
[12] I.R.M. Kottegoda, Y. Kadoma, H. Ikuta, Y. Uchimoto, M. Wakihara, Electrochem. Solid State Lett. 5 (2002) A275.
[13] E. Peled, C. Menachem, D. bar-Tow, A. Melman, J. Electrochem. Soc. 143 (1996) L4.
[14] Q.M. Pan, K.K. Guo, L.Z. Wang, S.B. Fang, J. Electrochem. Soc. 149 (2002) A1218.
[15] Y.K. Choi, K.I. Chung, W.S. Kim, Y.E. Sung, S.M. Park, J. Power Sources 104 (2002) 132.
[16] T. Tsumura, A. Katanosaka, I. Souma, T. Ono, Y. Aihara, J. Kuratomi, M. Inagaki, Solid State Ionics 135 (2000) 209.
[17] S.S. Zhang, K. Xu, T.R. Jow, J. Power Sources 129 (2004) 275.
[18] A Sano, M. Kurihara, K. Ogawa, T. Iijima, S. Maruyama, J. Power Sources 192 (2009) 703.
[19] Y.S. Park, H.J. Bang, S.M. Oh, Y.K. Sun, S.M. Lee, J. Power Sources 190 (2009) 553.
[20] D. Aubach, Y. Ein-Eli, B. Markovsky, A. Zaban, J. Electrochem. Soc. 142 (1995) 2882.
[21] Y. Ein-Eli, S.R. Thomas, V.R. Koch, J. Electrochem. Soc. 144 (1997) 1159.
[22] O. Matsuoka, A. Hiwara, T. Omi, M. Toriida, T. Hayashi, C. Tanaka, Y. Saito, T. Ishida, H. Tan, S.S. Ono, S. Yamamoto, J. Power Sources 119–121 (2003) 368.
[23] D. Aubach, K. Gamolsky, B. Markovsky, Y. Gofer, M. Schmidt, U. Heider, Electrochim. Acta 47 (2002) 1423.
[24] P. Yu, J.A. ritter, R.E. White, B.N. Popov, J. Electrochem. Soc. 147 (2000) 1280.
[25] S.S. Zhang, M.S. Ding, K. Xu, J. Allen, T.R. Jow, Electrochem. Solid State Lett. 4 (2001) A206.
[26] S.S. Zhang, K. Xu, T.R. Jow, J. Power Sources 115 (2003) 137.
[27] N. Ohzuku, Y. Iwakoshi, K. Sawai, J. Electrochem. Soc. 142 (1995) 371.
[28] T. Piao, S.M. Park, C.H. Doh, S.I. Moon, J. Electrochem. Soc. 146 (1999) 2794.
[29] Y.C. Chang, J.H. Jong, G.T. Fey, J. Electrochem. Soc. 147 (2000) 2033.
[30] X.G. Sun, C.A. Angell, Electrochem. Commun. 11 (2009) 1418.
[31] T.S. Ong, H. Yang, Electrochem. Solid State Lett. 4 (2001) A194.